JOC Article

Facile Ketene−Ketene and Ketene−Ketenimine Rearrangements: A Study of the 1,3-Migration of α-Substituents Interconverting α-Imidoylketenes and α-Oxoketenimines, a Pseudopericyclic Reaction

Justin J. Finnerty*,† and Curt Wentrup*

Department of Chemistry, School of Molecular and Microbial Sciences, The University of Queensland, Brisbane, Qld 4072, Australia

j.finnerty@uq.edu.au; wentrup@uq.edu.au

Received September 28, 2003

Theoretical calculations (B3LYP/6-311+G(3df,2p)//B3LYP/6-31G*) of the 1,3 migration of NR_2 transforming α-oxoketenimines **1** to α-imidoylketenes **3** and vice versa indicate that this process is a pseudo-pericyclic reaction with a low activation energy (NH_2 97 kJ mol^{-1}, $N(CH_3)_2$ 62 kJ mol^{-1}). The oxoketenimines were found to be more stable (by 18−35 kJ mol^{-1}) which is in line with experimental observations. The hindered amine rotation in the amide and amidine moieties adjacent to the cumulenes are important in the migration of the NR_2 group, as one of the rotation transition states is close to the 1,3 migration pathway. This gives an interesting potential energy surface with a valley-ridge inflection (VRI) between the orthogonal hindered amine rotation and 1,3 migration transition states. The imidoylketene may also undergo ring closure to an azetinone **5**; however, this is metastable, and under the conditions that allow the 1,3-migration, the oxoketenimine **1** will be favored. The imine NH *E*/*Z*-interconversion of the ketenimine group takes place by inversion and has a low activation barrier (∼40 kJ mol^{-1}). In all the amidines examined the *E*/*Z*-interconversion of the imine function was predicted to be by rotation with a high barrier (>80 kJ mol^{-1}), in contrast to all other reported imine *E*/*Z*-interconversions which are by inversion.

Introduction

There has been considerable recent experimental interest in the chemistry of α-oxoketenimines **1** and α-imidoylketenes[1,2] **3** and their interconversion via 1,3-substituent migration (Scheme 1).[3] They have also been the objects of several theoretical studies.[4−7] Although suprafacial thermal 1,3-migrations are formally "forbidden",[8] such migrations become possible in cumulenes.[3a,5−7] For instance, we recently[9] described the degenerate thermal 1,3 migration of the chloro-substituent of an α-oxoketene and determined the activation barrier, using

SCHEME 1

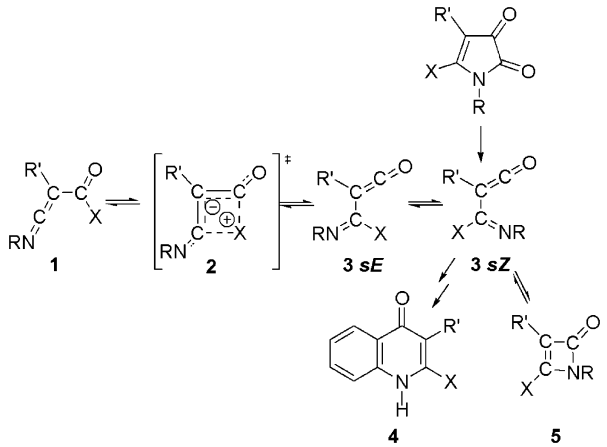

a X = R = R' = H
b X = OCH_3; R = phenyl; R' = H
c X = CH_3; R = 1'-adamantyl; R' = phenyl
d X = NH_2; R = R' = H
e X = $N(CH_3)_2$; R = R' = H

† Present address: Division of Chemical and Environmental Engineering, Faculty of Engineering, Physical Sciences and Architecture, The University of Queensland, Brisbane, Qld 4072, Australia

(1) (a) Piper, J. U.; Allard, M.; Faye, M.; Hamel, L.; Chow, V. *J. Org. Chem.* **1977**, *42*, 4261−4262. (b) Wentrup, C.; Ramana Rao, V. V.; Frank, W.; Fulloon, B. E.; Moloney, D. W. J.; Mosandl, T. *J. Org. Chem.* **1999**, *64*, 3608−3619.

(2) Wolf, R.; Wong, M. W.; Kennard, C. H. L.; Wentrup, C. *J. Am. Chem. Soc.* **1995**, *117*, 6789−6790. Wolf, R.; Stadtmüller, S.; Wong, M. W.; Barbieux-Flammang, M.; Flammang, R.; Wentrup, C. *Chem. Eur. J.* **1996**, *2*, 1319−1329.

(3) (a) Wentrup, C.; Netsch, K.-P. *Angew. Chem, Int. Ed. Engl.* **1984**, *23*, 802. (b) Wentrup, C.; Fulloon, B. E.; Moloney, D. W. J.; Bibas, H.; Wong, M. W. *Pure Appl. Chem.* **1996**, *68*, 891−894.

(4) Nguyen, M. T.; Ha, T.-K.; More O'Ferrall, R. A. *J. Org. Chem.* **1990**, *55*, 3251−3256.

(5) (a) Ham, S.; Birney, D. M. *J. Org. Chem.* **1996**, *61*, 3962−3968. (b) Zhou, C.; Birney, D. M. *J. Am. Chem. Soc.* **2002**, *124*, 5231.

(6) Wong, M. W.; Wentrup, C. *J. Org. Chem.* **1994**, *59*, 5279−5285.

(7) Koch, R.; Wong, M. W.; Wentrup, C. *J. Org. Chem.* **1996**, *61*, 6809−6813.

(8) Woodward, R. B.; Hoffmann, R. *The Conservation of Orbital Symmetry;* Academic Press: New York and Verlag Chemie: Weinheim, 1970.

(9) Finnerty, J.; Andraos, J.; Yamamoto, Y.; Wong, M. W.; Wentrup, C. *J. Am. Chem. Soc.* **1998**, *120*, 1701−1704.

10.1021/jo035419x CCC: $27.50
Published on Web 02/21/2004

TABLE 1. Calculated (B3LYP/6-311+G(3df,2p)//B3LYP/6-31G*) Energy Data[20] for the 1,3 Migration in α-Oxoketenes 6 Compared to the G2(MP2, SVP) Values (Difference Columns)[9] (Calculated Energy Values Are for 298.15 K)

	B3LYP			G2(MP2, SVP)	
compd/substituent[a]	$\Delta H^{\ddagger}$/kJ mol^{-1}	$\Delta S^{\ddagger}$/JK^{-1} mol^{-1}	$\Delta G^{\ddagger}$/kJ mol^{-1}	ΔE/kJ mol^{-1}	difference/kJ mol^{-1}
6b/N(CH$_3$)$_2$[a]	30.9	−20.6	37.0		−3.1
6b/N(CH$_3$)$_2$[b]	36.3	−23.7	43.3	34	−9.5
6c/Br	25.5	−18.1	30.9	37	8.0
6d/SH	39.9	−20.4	46.0	51	5.5
6e/Cl	37.6	−16.3	42.5	53	10.2
6a/NH$_2$	69.5	−11.8	73.1	70	−3.5
6f/F	78.7	−17.2	83.9	89	5.0
6g/OH	107.1	−14.2	111.4	114	3.1
6h/H	137.3	−10.1	140.3	143	2.4
6i/CH$_3$	198.2	−11.6	201.7	206	4.3

[a] In the N(CH$_3$)$_2$ case, the symmetric 1,3 migration structure was an intermediate. The migration therefore had two unsymmetric degenerate transition states either side of the intermediate. The results for both the intermediate ([a]) and the transition state ([b]) are reported.

dynamic NMR (T_C −29 °C) or density functional theory (DFT) calculation, to be ∼40 kJ mol^{-1} (eq 1).

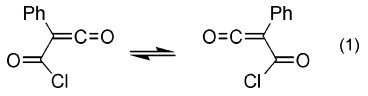

(1)

It is known that reactions producing methylthio-, dimethylamino-, or alkoxyimidoylketenes **3** can give rise to products derived from the corresponding 1,3-migration partner, the oxoketenimines **1**.[10] The reverse process has also been demonstrated, e.g., the flash vacuum thermolysis (FVT) of **1b** affording the cyclization product of the corresponding α-imidoylketene, the 4-quinolone **4b** (94% yield by FVT at 800 °C).[11] While **1b** was the major heterocumulene product after FVT, with a 10-fold greater intensity of its cumulene band in the infrared region 2000−2200 cm^{-1}, a dynamic equilibrium must have existed to account for the high yield of **4b** (calculated intensity ratios for isomeric imidoylketenes and oxoketenimines are of the order 750:450 km mol^{-1}; representative data are given in the Supporting Information). In competition with the 1,3-migration there is a reversible electrocyclic ring closure of **3** to form **5**. This ring closure has been reported both experimentally[12] (**3c** to **5c**) and theoretically[4] (**3a** to **5a**). The alternative ring closure to form an imino-oxetene has previously been calculated[4] to be unstable and was not considered here. So far, only one ab initio study of the 1,3-migration process in oxoketenimines/imidoylketenes has been reported,[5a] predicting a 1,3-migration barrier of 200 kJ mol^{-1} for the hydrogen migration in the parent α-imidoylketene (at MP4(FC, SDQ)/6-31G* + ZPVE). In their study of the ring closure to **5a**, Nguyen and co-workers[4] calculated an activation barrier of 102 kJ mol^{-1} (MP4(SDQ)/6-31G** + ZPVE), with the monocyclic **5a** being 41 kJ mol^{-1} less stable than **3a**.

The migratory aptitude of a range of substituents was studied previously for the α-oxoketene system **6** (eq 2).[6,9] For ease of comparison with the present study, the migratory aptitudes of oxoketenes **6** have been recalculated at the DFT level used here, and the data are presented in Table 1.

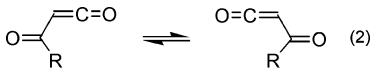

(2)

6 **a** R = NH$_2$ **b** R = NMe$_2$ **c** R = Br **d** R = SH **e** R = Cl **f** R = F **g** R = OH **h** R = H **i** R = CH$_3$

The imidoylketene/oxoketenimine system can be expected to behave in a manner qualitatively similar to that of **6**. The amino and dimethylamino substituents have been found to be very good migrating groups in both experiment and calculations (calculated barriers for NH$_2$ 70 and for N(CH$_3$)$_2$ 34 kJ mol^{-1} in **6**). Furthermore, the dimethylamino group migration in **6b** was uniquely found to present a shallow minimum for the four-membered cyclic zwitterionic intermediate **7** (eq 3).[6]

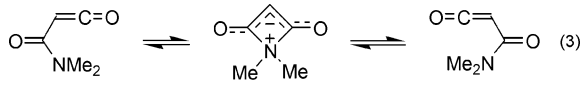

(3)

6b **7** **6b**

With amino migrating groups, three other conformational changes may impact on the migration. First, the amidine or amide group may rotate about the single bond to the heterocumulene (*sE*,[13] *sZ*, *s90*, *s270*, rotation A, Scheme 2). Second, the amino group may undergo hindered rotation about the carbon−nitrogen bond (*A0*,[13] *A90*, *A180*, rotation B, Scheme 2). The imine functions on the amidine may undergo rotation or inversion of the nitrogen substituent (imine *IZ*[13] and *IE*, linear transition state *IL*, and rotation transition state *IR*, rotation/Inversion C, Scheme 2). Likewise, the ketenimine imine functions may undergo rotation or inversion of the nitrogen substituent (imine *kI90*[13] and *kI270*, linear transition state *kIL*, and rotation transition state *kIR*, rotation/inversion D, Scheme 2).

In the previous study[6] of the α-oxoketenes **10**, two minima were found for the α-amide group rotating about the single bond to the heterocumulene with both minima coplanar with the cumulene (*sE* and *sZ*). In that study, the relative energies between the two minima were −2 to +5 kJ mol^{-1} with rotation barriers of 26−41 kJ mol^{-1}

(10) Ben Cheikh, A.; Chuche, J.; Manisse, N.; Pommelet, J. C.; Netsch, K.-P.; Lorençak, P.; Wentrup, C. *J. Org. Chem.* **1991**, *56*, 970−975.

(11) (a) Fulloon, B.; El-Nabi, H. A. A.; Kollenz, G.; Wentrup, C. *Tetrahedron Lett.* **1995**, *36*, 6547−6550. (b) Fulloon, B. E.; Wentrup, C. *J. Org. Chem.* **1996**, *61*, 1363−1368. (c) Clarke, D.; Mares, R. W.; McNab, H. *J. Chem. Soc., Perkin Trans. 1* **1997**, 1799−1804.

(12) Kappe, C. O.; Kollenz, G.; Netsch, K.-P.; Leung-Toung, R.; Wentrup, C. *J. Chem. Soc., Chem. Commun.* **1992**, 488−490.

SCHEME 2

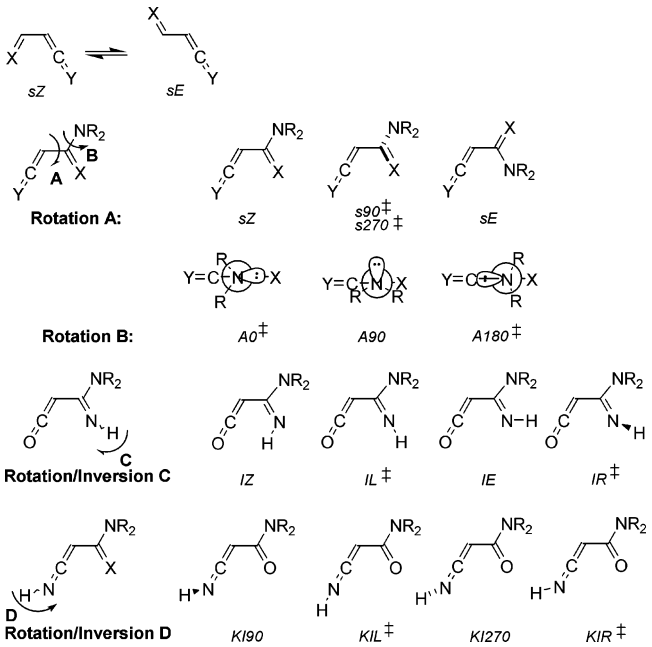

for all the substituents studied.[6,9] The difference in relative stabilities of the two minima conformers of α-amino-α-oxoketene **6a** was 5 kJ mol^{-1} with an *E*/*Z* rotation barrier of 26 kJ mol^{-1}. It was to be expected that two similar conformers of the amido or amidino functions of **1** and **3** would be minima. As the 1,3-migration may only occur from one of these orientations (*sE*), the rotation between, and the relative stabilities of the two minima was of interest.

The hindered rotation of nitrogen in amides is important, since the migrating amino group must go from the hindered rotation ground state (A90) to one of the rotation transition states (A180) before the lone pair points toward the heterocumulene. Much work has been carried out on the hindered rotation of nitrogen in amides; for instance, the rotation barriers have been determined experimentally for *N*,*N*-dimethylformamides **9** (rotation B in **9**; Scheme 3: **9a** 89 (ref 14), **9b** 66, **9c** 70, **9d** 73, **9e** 77, and **9f** 91 kJ mol^{-1}).[15] The presence of

SCHEME 3

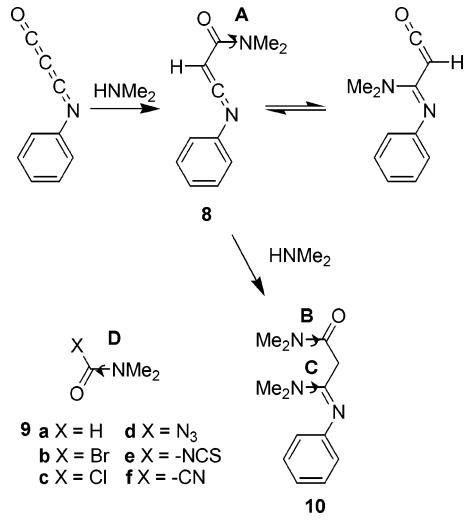

the heterocumulene in α-oxoketenimines lowers the rotation barrier of the nitrogen in the amide group of **6** (From dynamic NMR experiments; rotation A = 54−57;[16] rotation B = 77 for the amide nitrogen,[16] and rotation C = 46 kJ mol^{-1} for the amidine nitrogens[16] of **8** and **10**). This is not observed with the other heterocumulene groups, viz. azide (**9d**)[15] or isothiocyanate (**9e**, Scheme 3).[15] The rotation barrier of the nitrogen in *N*,*N*-dimethylformamide and the α-oxoketenimines is higher than the calculated 1,3-migration barrier for the dimethylamino group in α-oxoketene (**6b** 34 kJ mol^{-1}, Table 1).[9] The relevance of this will be discussed below.

Imino groups can exist in *E* and *Z* forms. It has been reported that the conversion between these *E* and *Z* conformers occurs via inversion of the ketenimine[17,18] or imine[19] nitrogen. Jochims and co-workers[18] determined inversion barriers of 30−65 kJ mol^{-1} for ketenimines, while Knorr and co-workers[19] determined inversion barriers of 57−64 kJ mol^{-1} for imines. The latter found no *rotation* about the imine nitrogen up to the maximum temperature studied, thus indicating that if such a process occurred its activation barrier was greater than 96 kJ mol^{-1}. The imine and ketenimine NH inversions are described by rotations/inversions C and D in Scheme 2. It has been shown elsewhere that electronegative substituents on C can cause ketenimines to become linear along the CCN−R chain;[2,17] i.e., the nitrogen inversion barrier can decrease to zero.

Previous DFT calculations (using the theory and basis-set used here) of the 1,3-migration barrier for chlorine in α-oxoketenes (eq 1) was in good agreement with the experimentally determined value.[9] DFT calculations (again using the theory and basis-set used here) on linear ketenimines[17] were also in good agreement with experiment. Therefore, DFT calculations on the α-oxoketen-

(13) The following labeling system is used to differentiate the conformers. The conformations of the amide and amidine groups with respect to the cumulene function (rotation A, Scheme 2) are denoted by "*sZ*" and "*sE*" (planar) with, "*s90*" and "*s270*" representing the dihedral angle between the highest priority groups (*sZ* ≡ "*s0*" and *sE* ≡ "*s180*"). To denote the position of the amine nitrogen, the nitrogen's lone pair was considered the most relevant feature; accordingly the dihedral angle between the lone pair and the adjacent heteroatom was used. The position of the lone pair was estimated as halfway between the two hydrogens and on the opposite side of the nitrogen atom. Rotation **B**, Scheme 2 is denoted as "*A0*", "*A90*", and "*A180*". The "*A270*" is equivalent to "*A90*" either by symmetry or by inversion of the ketenimine nitrogen and has not been used. The position of the imine hydrogen (rotation/inversion C, Scheme 2) is denoted by "*IZ*" or "*IE*" for the *Z* or *E* conformers of the amidine imine, "*IL*" for the linear inversion transition state, and "*IR*" for the rotation transition state. For the ketenimine function (rotation/inversion D, Scheme 2) "*kI90*" or "*kI270*" represent the dihedral angle between the ketenimine NH bond and the carbon substituent on the heterocumulene, "*kIL*" is the linear inversion transition state, and "*kIR*" the rotation transition state. When discussing structures, a composite label may be abbreviated if the conformations of the unspecified parts are supplied by the context.

(14) Sandström, J. *Dynamic NMR Spectroscopy;* Academic Press: London, 1982; Chapter 7, p 119.

(15) Allan, E. A.; Hobson, R. F.; Reeves, L. W.; Shaw, K. N. *J. Am. Chem. Soc.* **1972**, *94*, 6604−6611.

(16) Wentrup, C.; Rao, V. V. R.; Frank, W.; Fulloon, B. E.; Moloney, D. W. J.; Mosandl, T. *J. Org. Chem.* **1999**, *64*, 3608−3619.

(17) Finnerty, J.; Mitschke, U.; Wentrup, C. *J. Org. Chem.* **2002**, *67*, 1084−1092.

(18) (a) Jochims, J. C.; Lambrecht, J.; Burkert, U.; Zsolnai, L.; Huttner, G. *Tetrahedron* **1984**, *40*, 893−905. (b) Lambrecht, J.; Gambke, B.; von Seyerl, J.; Huttner, G.; Kollmannsberger-von Nell, G.; Herzberger, S.; Jochims, J. C. *Chem. Ber.* **1981**, *114*, 3751−3773.

(19) Knorr, R.; Ruhdorfer, J.; Mehlstäuble, J.; Böhrer, P.; Stephenson, D. S. *Chem. Ber.* **1993**, *126*, 747−754 and references therein.

TABLE 2. Calculated (B3LYP/6-311+G(3df,2p)//B3LYP/6-31G*) Thermochemistry for the 1,3 Migration and the Ring Closure (Scheme 1)[a]

	amidine *IE*			amidine *IZ*		
	ΔH/kJ mol^{-1}	ΔS/JK^{-1} mol^{-1}	ΔG/kJ mol^{-1}	ΔH/kJ mol^{-1}	ΔS/JK^{-1} mol^{-1}	ΔG/kJ mol^{-1}
			NH_2 1,3 Migration[b]			
3d *sE-A90*	0.0	0.0	0.0	0.0	0.0	0.0
3d *sE-A180*‡	25.4	−8.4	27.9	22.7	−10.5	25.8
2d transition state	109.0	−13.9	113.2	92.5	−14.5	96.8
1d *sE-A180-kI90*‡	28.2	−6.8	30.2	22.5	−9.0	25.2
1d *sE-A90-kI90*	−17.5	3.1	−18.4	−23.1	0.8	−23.3
			$N(CH_3)_2$ 1,3 Migration[b]			
3e *sE-A90*	0.0	0.0	0.0	0.0	0.0	0.0
3e *sE-A180*‡	17.0	−20.0	23.0	12.5	−19.5	18.3
2e transition state	74.5	−14.3	78.7	57.4	−14.9	61.9
1e *sE-A180-kI90*‡	21.3	−18.6	26.8	13.2	−17.3	18.3
1e *sE-A90-kI90*	−15.3	6.1	−17.1	−23.4	7.4	−25.6
			Ring Closure[c]			
5d				31.7	−18.1	37.1
ring closure t.s.				50.9	−14.8	55.4
3d *sZ-A90*				−2.4	1.5	−2.9
3d *sE-A90*				0.0	0.0	0.0

[a] The thermochemistry values are for 298.15 K. [b,c] For the 1,3 migration, the values are relative to the **3d**/**3e** *sE-A90* conformers, and for the ring closure they are relative to the **3d** *sE-A90-IZ* conformer.

imine-α-imidoylketene system are expected to yield reliable results.

Results and Discussion

Two energy minima for the amide or amidine group rotations (rotation A, Scheme 2), amine rotation (rotation B, Scheme 2) and two for the imine inversion (imine Inversion/rotation C and ketenimine inversion D, Scheme 2) were calculated. Also of interest were the transition structures for the amide or amidine rotations (rotation A, Scheme 2), the hindered amine rotations (rotation B, Scheme 2), the imine inversions (imine inversion/rotation C and ketenimine inversion D, Scheme 2), and the 1,3-migration pathways for both the amino and dimethylamino series. For comparison, computational results for a series of compounds including conjugated and unconjugated amides or amidines were used, namely α-amidoketene **6a**, formamide **9a**, cyanoformamide **9f**, acrylamide **11**, formamidine **12**, and acrylamidine **13**.

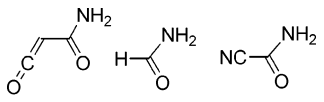

The equilibrium geometries were calculated for the two imine conformers of both of the ketenes (amidine *IE*/*IZ* NH_2 **3d**, $N(CH_3)_2$ **3e**) and the ketenimines (ketenimine *kI90*/*kI270* NH_2 **1d**, $N(CH_3)_2$ **1e**.) The two ketenimine conformers (*kI90* and *kI270*) have equal energy, and so only the *kI90* conformer was used in further calculations. The ketene amidine *IZ* and *IE* conformers are not identical, the imine *Z* form being lower in energy. Thus, one ketenimine and two ketene conformers were used as the base geometry for the study of the hindered amine rotation and the amide/amidine group (*sE*/*sZ* isomerization) rotations. The relative energies for the various conformation changes have been placed in Table 2 for the 1,3-migration, Table 3 for the amide/amidine group rotation, Table 4 for the hindered amine rotation, Table 5 for the imine nitrogen inversion/rotation, and Table 6 for the ketenimine nitrogen inversion. The four 1,3-migrations are illustrated in Figure 1, and a plot of the potential energy surface of the pathway for the 1,3-migration between **3d** *IZ* and **1d** *kI90* is presented in Figure 2 (similar graphs for the other three migration paths are placed in the Supporting Information).

Key harmonic vibrations and intensities, calculated total energy, ZPVE and dipole moments, key optimized structural parameters for all the conformers and structures have been summarized in tables and figures in the Supporting Information. Additionally, the complete harmonic vibrations and infrared intensities, as well as optimized geometries and imaginary frequencies for transition states are also available in the Supporting Information.

The α-oxoketenimines (**1d/e**) were calculated to be more stable than the corresponding α-imidoylketenes (**3d/e**), by 17−26 kJ mol^{-1}. This would suggest that at the FVT temperature of 650 K (380 °C) the ratio of ketenimine to ketene would be about 40:1, which is the sort of magnitude observed experimentally by infrared spectroscopy.[11]

Two ground-state conformers (*sE*/*sZ*, rotation A, Scheme 2) were found for the ketenimines (**1d**/**e**) and two for each of the *IE* and *IZ* conformers of the amidine groups in the imidoylketenes (**3d**/**e**). The *sE*/*sZ* energies for all the NH_2- and $N(CH_3)_2$-substituted species were not significantly different (energy differences are: NH_2 in **1d** 0.5, in **3d** *IE* 4.2 and in *IZ* 2.9 kJ mol^{-1}; $N(CH_3)_2$ in **1e** 9.6, in **3e** *IE* 0.3 and in *IZ* 6.1 kJ mol^{-1}). The NH_2 amide and *IZ* amidine (*IE* case not calculated) groups both have the same calculated rotation barrier of 24 kJ mol^{-1} (see Table **3**). These group rotation barriers are similar to the previously reported[7] calculations for α-oxoketenes **6** (NH_2 26; $N(CH_3)_2$ 24 kJ mol^{-1}, with 14−41 kJ mol^{-1} for all

TABLE 3. Calculated (B3LYP/6-311+G(3df,2p)//B3LYP/6-31G*) Thermochemistry for the *sE/sZ* Rotation (Rotation A, Scheme 2)[a]

	Amidine Groups											
	3d *IZ*				**13** *IE*				**13** *IZ*			
	sZ	*s90*	*sE*	*s270*	*sZ*	*s90*	*sE*	*s270*	*sZ*	*s90*	*sE*	*s270*
ΔH/kJ mol^{-1}	−2.4	20.1	0.0	20.0	0.0	5.2	−3.4	16.7	0.0	12.7	−2.5	13.0
ΔS/JK^{-1} mol^{-1}	1.5	−11.6	0.0	−12.2	0.0	−11.3	−2.3	−10.5	0.0	−13.2	−3.9	−12.2
ΔG/kJ mol^{-1}	−2.9	23.5	0.0	23.6	0.0	8.6	−2.7	19.9	0.0	16.6	−1.4	16.6

	Amide Groups							
	1d *kI90*				**11**			
	sZ	*s90*	*sE*	*s270*	*sZ*	*s90*	*sE*	*s270*
ΔH/kJ mol^{-1}	−0.4	23.8	0.0	20.5	−6.2	9.6	0.0	9.6
ΔS/JK^{-1} mol^{-1}	0.4	−5.6	0.0	−10.1	3.9	−8.9	0.0	−8.9
ΔG/kJ mol^{-1}	−0.5	25.4	0.0	23.5	−7.4	12.3	0.0	12.3

[a] The ΔG energies listed here are calculated relative to the most stable conformer. The energy values are for 298.15 K. All calculations reported in this table were performed at the hindered amine rotation ground state (*A90*).

substituents, see Table 1**)**. The group rotation barriers for the conjugated acrylic acid derivatives studied were slightly lower than for the heterocumulenes (acrylamide **11**: 12, and acrylamidine **13** *IE:* 9 kJ mol^{-1}; **13** *IZ:* 17 kJ mol^{-1}). This indicates that the effect of the heterocumulene on the amide/amidine group rotation is an increase of ∼10 kJ mol^{-1} above the effect of a conjugated double bond, probably due to stronger conjugation with the more polar heterocumulenes. The rotation barriers between these conformers is well below the 1,3-migration barrier, thus rendering this rotation A chemically unimportant with regard to the 1,3-migration, as the molecule can access the required *sE* conformer well before it has enough energy to undergo the migration.

For the hindered amine rotation (rotation B, Scheme 2) two minima were predicted, both when the nitrogen lone pair is normal to the N−C═X plane (*A90*, *A270*), with two corresponding maxima when the lone pair is in this plane (*A0*, *A180*). In general, the maxima with the higher energies occurred when the nitrogen lone pair was pointing toward the adjacent C═X bond (*A0*), more so in the *sE* than the *sZ* conformers. The nitrogen lone pair pointing toward the heterocumulene in the *sE* (*A180*) structures may account for the stabilization of this conformer. The predicted barriers for the hindered amine rotation (44−61 kJ mol^{-1}) of heterocumulene amides (NH_2 and $N(CH_3)_2$) encompass the values reported for this rotation[16] (amide **6** 54−57 kJ mol^{-1}, Scheme 3). They are smaller than the calculated value for formamide **9a** (78 kJ mol^{-1}) and cyanoformamide **9f** (76 kJ mol^{-1}), but are similar to the conjugated acrylamide **11** (54, 67) calculated. The difference of ∼10 kJ mol^{-1} between the calculated and experimental rotation barriers for **9a** (78 versus 89) and **9f** (76 versus 91 kJ mol^{-1}) is within the estimated accuracy of the computational method (∼12 kJ mol^{-1}, vide infra). Note also that the experimental results derive from solution phase experiments. The range of calculated results for the hindered amine rotation in amidines (**3d**: 26−39 kJ mol^{-1} and **3e**: 18−40 kJ mol^{-1}) was below the calculated values for the unconjugated formamidine **12** (52 (*IE*) and 41 (*IZ*) kJ mol^{-1}), but close to those for the conjugated acrylamidine **13** (33−45 kJ mol^{-1}) compounds. Additionally, a small reduction of <6 kJ mol^{-1} is observed for this barrier when going from the *IE* to the *IZ* conformers; this difference may be due to greater steric crowding in the *IZ* imine conformation. The hindered amine rotation barrier of a conjugated amide or amidine was ∼10 kJ mol^{-1} lower than for the unconjugated systems. This may be explained by the satisfaction of the carbonyl electron demand by conjugation and is not specific to the heterocumulene system.

As mentioned above, the *A180* transition state is generally of lower energy than the corresponding *A0* conformer. Unfavorable electron repulsion between the nitrogen lone pair and the adjacent imine bond may provide an explanation. The exceptions to this are seen in some of the *IE* amidine conformers, where the imine hydrogen points toward the amine nitrogen. The position of this imine hydrogen may provide a hydrogen bond in the *IE-A0*, and sterically hinder the amine hydrogens in the *IE-A180* conformers.

Interestingly, when a heterocumulene is present the magnitude of the energy difference between the *A180* and *A0* transition states is larger in the *sE* than the *sZ* conformation, and the distance between the amino nitrogen and the central carbon of the heterocumulene is shorter than any other point (2.6 vs >2.8 Å for the α-imidoylketenes and 2.75 vs >2.85 Å for the α-oxoketenimines). The reduction in distance is caused by compression of the NC_1C_2 angle by about 3° and not by changes in the bond lengths, indicating an attraction between the nitrogen and the central heterocumulene carbon rather than changes in conjugation of the amide/amidine. The changes in geometry suggest that an interaction between the nitrogen lone pair and the heterocumulene LUMO causes the (up to 22 kJ mol^{-1}) decrease in the energy of the sE-A180 conformer. This interaction could suggest that the sE-A180 conformers are pre-transition states in the process of the 1,3-migration. This hypothesis is supported by the reaction path calculations (vide infra and Figure 2) that show these rotation transition structures are close to the 1,3-migration pathway.

The inversion barrier for the ketenimine nitrogen (inversion D, Scheme 1) was calculated as 42 kJ mol^{-1} for the *sE-A90-kIL* and 35 kJ mol^{-1} for the *sZ-A90-kIL* conformer. These values are at the lower end of the reported range and in accord with findings for linear ketenimines, where electron-withdrawing groups on the ketenimine carbon reduced the barrier.[17] No corresponding transition state *kIR* for rotation D was found. The

TABLE 4. Calculated (B3LYP/6-311+G(3df,2p)//B3LYP/6-31G*) Thermochemistry for the Hindered Amine Rotation (Rotation B, Scheme 2) in the Amides and Amidines Relative to the *A90* Conformer[a]

Amides

	1d *kI90*				**1e** *kI90*			
	sE		*sZ*		*sE*		*sZ*	
	A0	*A180*	*A0*	*A180*	*A0*	*A180*	*A0*	*A180*
ΔH/kJ mol^{-1}	62.9	45.7	65.8	53.1	60.9	36.5	62.3	52.4
ΔS/JK^{-1} mol^{-1}	−7.6	−9.8	−6.4	−7.6	−21.8	−24.7	−26.4	−27.2
ΔG/kJ mol^{-1}	65.2	48.6	67.7	55.4	67.4	43.9	70.1	60.5

	10a *sE*	
	A0	*A180*
ΔH/kJ mol^{-1}	59.1	35.7
ΔS/JK^{-1} mol^{-1}	−8.8	−12.2
ΔG/kJ mol^{-1}	61.7	39.3

	9a		**9f**		**11**			
					sE		*sZ*	
	A0	*A180*	*A0*	*A180*	*A0*	*A180*	*A0*	*A180*
ΔH/kJ mol^{-1}	77.8	73.2	74.9	73.5	66.0	51.6	74.8	63.9
ΔS/JK^{-1} mol^{-1}	−17.1	−16.7	−8.4	−9.3	−8.0	−9.5	−8.6	−10.0
ΔG/kJ mol^{-1}	82.9	78.3	77.4	76.3	68.4	54.4	77.4	66.9

Amidines

	3d							
	sE				*sZ*			
	IE		*IZ*		*IE*		*IZ*	
	A0	*A180*	*A0*	*A180*	*A0*	*A180*	*A0*	*A180*
ΔH/kJ mol^{-1}	47.4	25.4	27.6	22.7	51.3	37.4	31.6	34.6
ΔS/JK^{-1} mol^{-1}	−4.8	−8.4	−7.6	−10.5	−0.8	−5.2	−6.7	−8.4
ΔG/kJ mol^{-1}	48.9	27.9	29.9	25.8	51.5	38.9	33.6	37.0

	3e							
	sE				*sZ*			
	IE		*IZ*		*IE*		*IZ*	
	A0	*A180*	*A0*	*A180*	*A0*	*A180*	*A0*	*A180*
ΔH/kJ mol^{-1}	44.3	17.0	34.7	12.5	41.8	34.7	24.3	28.7
ΔS/JK^{-1} mol^{-1}	−17.5	−20.0	2.2	−19.5	−16.8	−17.8	−17.1	−19.0
ΔG/kJ mol^{-1}	49.6	23.0	34.1	18.3	46.8	40.0	29.3	34.4

	12			
	IE		*IZ*	
	A0	*A180*	*A0*	*A180*
ΔH/kJ mol^{-1}	56.2	50.2	39.0	47.7
ΔS/JK^{-1} mol^{-1}	−4.8	−4.6	−5.5	−5.0
ΔG/kJ mol^{-1}	57.7	51.6	40.6	49.2

	13							
	sE				*sZ*			
	IE		*IZ*		*IE*		*IZ*	
	A0	*A180*	*A0*	*A180*	*A0*	*A180*	*A0*	*A180*
ΔH/kJ mol^{-1}	49.9	36.2	30.3	34.3	55.3	44.8	37.3	42.6
ΔS/JK^{-1} mol^{-1}	−5.9	−6.9	−7.3	−7.9	−3.3	0.5	−3.3	−5.6
ΔG/kJ mol^{-1}	51.6	38.2	32.5	36.7	56.2	44.7	38.3	44.3

[a] The ΔG energies listed here are calculated relative to the *A90* conformer. The energy values are for 298.15 K.

calculation for the inversion barrier of the imine nitrogen in the amidines failed to predict the expected linear transition structure (*IL*, inversion C, Scheme 2). Instead, all the amidines have the linear imine inversion conformer as a second-order saddle point (85−90 kJ mol^{-1}), and the rotation-like transition state (*IR*) for rotation C lies 81−92 kJ mol^{-1} above the ground state. Regardless of whether these amidine imines undergo inversion or rotation, both barriers are much higher than the reported range for other imines.[18,19] This finding seems unprecedented, as all reports point to an inversion mechanism for imine structures, although no study of amidine imine inversion has been reported. The difference in energy between the two ground-state imine conformers (both

TABLE 5. Calculated (B3LYP/6-311+G(3df,2p)//B3LYP/6-31G*) Thermochemistry for the Imine and N−H Inversions/ Rotations (Rotation C (IL and IR), Scheme 2)[a]

	formamidine **12**				amidinoketene **3d**							
					sE				*sZ*			
	IZ	*IL*[b]	*IR*	*IE*	*IZ*	*IL*[b]	*IR*	*IE*	*IZ*	*IL*[b]	*IR*	*IE*
ΔH/kJ mol^{-1}	0.0	83.7	86.0	−7.8	0.0	85.6	83.3	−5.6	−1.8	84.5	80.7	0.0
ΔS/JK^{-1} mol^{-1}	0.0	−2.2	4.0	−1.1	0.0	2.7	2.4	−2.3	1.1	−0.5	0.8	0.0
ΔG/kJ mol^{-1}	0.0	84.3	8.5	−7.5	0.0	84.8	82.6	−4.9	−2.2	84.7	80.5	0.0
	acrylamidine **13**							
	sE				*sZ*			
	IZ	*IL*[b]	*IR*	*IE*	*IZ*	*IL*[b]	*IR*	*IE*
ΔH/kJ mol^{-1}	0.0	94.2	92.9	−4.2	0.0	86.9	86.9	−3.3				
ΔS/JK^{-1} mol^{-1}	0.0	16.3	4.1	−0.8	0.0	−3.6	−1.2	−2.4				
ΔG/kJ mol^{-1}	0.0	89.3	91.6	−4.0	0.0	88.0	87.3	−2.6				

[a] The ΔG values listed here are calculated relative to the most stable conformer (*IE*) and were performed at the hindered amine rotation ground state (*A90*). The energy values are for 298.15 K. [b] These structures are second-order saddle points and have two imaginary frequencies.

TABLE 6. Calculated (B3LYP/6-311+G(3df,2p)//B3LYP/ 6-31G*) Thermochemistry for the Ketenimine N−H Inversion D (kIL) (Scheme 2)[a]

	ketenimine **1d**	
	sE	*sZ*
	kIL	*kIL*
ΔH/kJ mol^{-1}	42.1	35.1
ΔS/JK^{-1} mol^{-1}	1.0	−0.2
ΔG/kJ mol^{-1}	41.8	35.2

[a] The ΔG values listed here are calculated relative to the most stable conformer (*IE*) and were performed at the hindered amine rotation ground state (*A90*). The energy values are for 298.15 K.

amidines and ketenimines) was not significant (0−8 kJ mol^{-1}). The barriers for ketenimine NH inversion D (35 and 42 kJ mol^{-1}) are chemically unimportant, as they are below the interesting hindered amine rotation and 1,3-migration barriers. The barriers for amidine imine NH inversion/rotation C are however, comparable to the 1,3-migration barriers.

The calculated ring closure barrier to form the azetinone **5d** from the imidoylketene **3d** *sZ-A90-IZ* was 58 kJ mol^{-1}, which is lower than the corresponding 1,3-migration barrier. The ring structure **5d** is 40 kJ mol^{-1} less stable than **3d** *sZ-A90-IZ*, however, so the barrier to ring opening is only 18 kJ mol^{-1}. No calculation for the transition state of the *IE* case was performed but could be expected to be qualitatively similar to the *IZ* case, but with **5d** 38 kJ mol^{-1} less stable than **3d** *sZ-A90-IE*. Therefore, **5d** may be formed as a metastable compound under certain reaction conditions,[12] but under the conditions where the 1,3-migration is taking place, it would be only a small part of the equilibrium mixture.

The barrier to 1,3-migration in the α-oxoketenimine−α-imidoylketene system **1**/**3** is ∼30 kJ mol^{-1} more than that found in the α-oxoketene (**6**) system using the same computational method (see Table 1).[20] Interestingly, the difference in energy between the 1,3-migration transition state and both the ketenimine and ketene *sE-A180* amine rotation transition state conformers is about the same, namely ∼85 kJ mol^{-1} for the *IE* and ∼70 for the *IZ* NH_2 cases, and ∼55 for the *IE* and ∼45 kJ mol^{-1} for the *IZ* $N(CH_3)_2$ cases (see Figure 1). Therefore, the Hammond postulate might lead one to expect the 1,3-migration transition state to be close to the halfway point between the two rotation transition states.[21] This is close to what we calculated, with the transition states having a ketenimine-like backbone but with the imine NH somewhere between the in-plane *E*/*Z* imine and the 90° out-of-plane ketenimine geometries.

To satisfy ourselves that the transition states were for the 1,3-migrations and that an intermediate did not exist, intrinsic reaction path calculations (IRC) were performed (see Figure 2). Note that the graph (Figure 2A) has minor inflection points at about −6 and +4 units on the reaction coordinate. The dihedral angle shown for the NH_2 group (Figure 2B) will be 0° at the *sE-A90* ground state and 90° at the hindered amine transition state. The angle increases steadily toward 90° from the left until −6, then plateaus until +4 units when it starts returning to the ground state value. In contrast, the changes in (actual) bond lengths (Figure 2C,D) only occur between −6 and +4 units on the reaction coordinate. This indicates that these inflection points represent valley-ridge inflections[22] (VRI) on the potential energy surface. The energies of the VRI points (−60 to −80 kJ mol^{-1}) are close in energy to the hindered amine rotational transition states *sE-A180*. The calculated geometries and the energies both show these rotational transition states are close to the VRI points and mean the hindered amine rotation pathway is close to, or forms part of, the 1,3- migration pathway.[23]

Thus, it may be said that the first part of the activation barrier, up to the *sE-A180* rotamers in Figure 1 or to the inflection points in Figure 2 and about 18−28 kJ mol^{-1} above the imidoylketene reference point, is due to rota-

(20) Finnerty, J. J. *A Computational and Experimental Study of Heterocumulenes*. Ph.D. Thesis, The University of Queensland, Australia, 2001.

(21) Hammond, G. S. *J. Am. Chem. Soc.* **1955**, *77*, 334−338.

(22) Valtazanos, P.; Ruedenberg, K. *Theor. Chim. Acta* **1986**, *69*, 281−307. Konkoli, Z.; Kraka, E.; Cremer, D. *J. Phys. Chem.* A **1997**, *101*, 1742−1757. Cremer, D.; Wu, A.; Kraka, E. *Phys. Chem. Chem. Phys.* **2001**, *3*, 674−687. Bartsch, R. A.; Chae, Y. M.; Ham, S.; Birney, D. M. *J. Am. Chem. Soc.* **2001**, *123*, 7479−7486.

(23) The *IE* case follows a similar pattern (Figure S2, Supporting Information). In the case of the IRC calculations for the $N(CH_3)_2$ substituted ketene and ketenimine, the reaction coordinate was not extended sufficiently to reach the $N(CH_3)_2$ rotation stages of the transition path; however, the part of the migration path that was calculated follows the same pattern as in the NH_2 case.

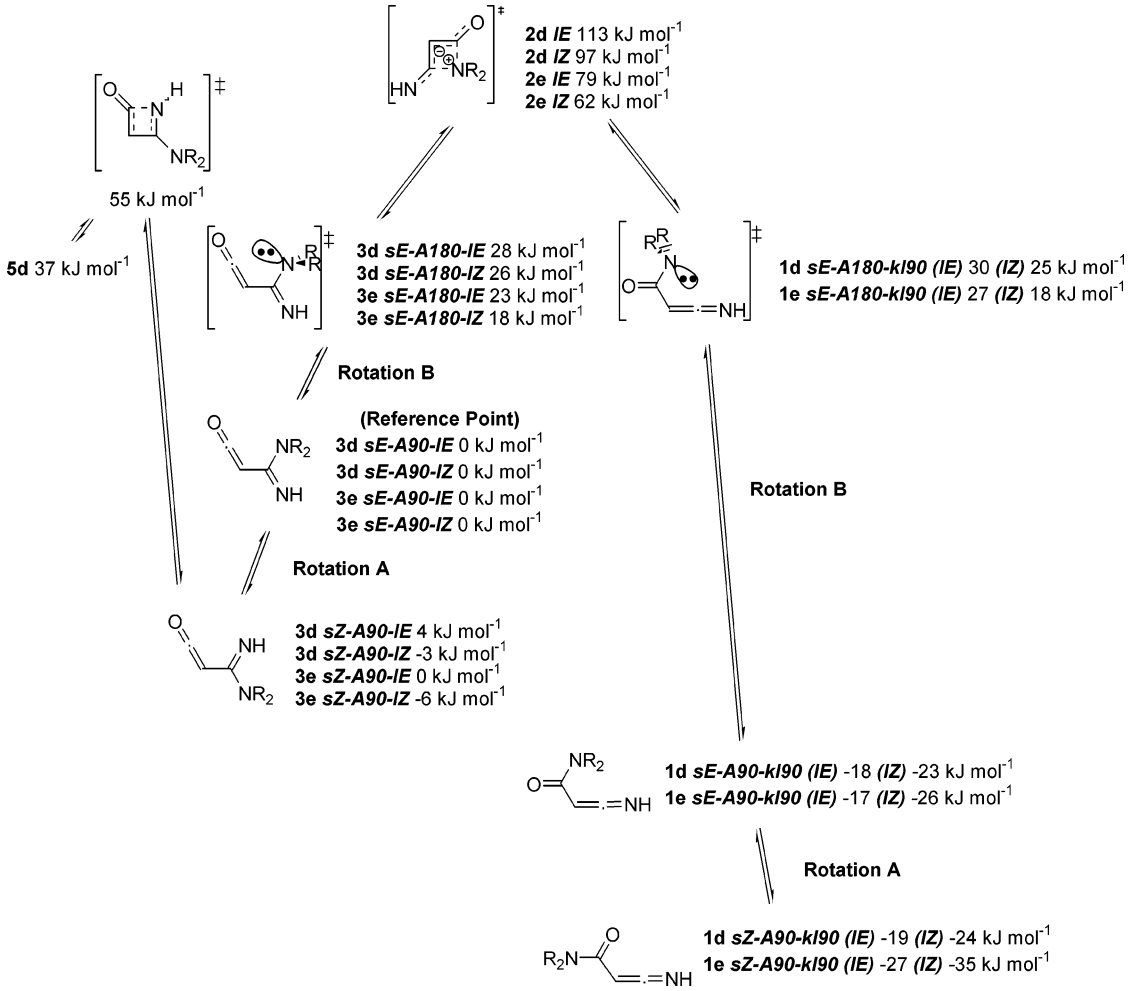

FIGURE 1. Summary of the calculated free energy (ΔG) changes for the NR_2 1,3-migrations **1e** to **3e** *IE* (R = methyl), **1e** to **3e** *IZ* (R = methyl), **1d** to **3d** *IE* (R = H), **1d** to **3d** *IZ* (R = H), and the ring closure of **3d** to azetinone **5d**. Energies in kJ mol^{-1} at the B3LYP/6-311+G(3df,2p)//B3LYP/6-31G* level. Only the *kI90* conformer of the ketenimines **1** has been calculated; the (*IE*) or (*IZ*) refers to the ketene **3** conformer used as the reference point. (Rotation A energies are **3d** *s90-A90-IZ* 23.5; **1d** *s90-A90-kI90* 25.4 kJ mol^{-1}.)

tion of the amino group into the correct orientation for the 1,3-migration. At this point, the amine lone pair is pointing toward the in-plane π orbital at the central carbon atom of the ketene or ketenimine. The DFT-calculated molecular orbitals of the *sE-A180* conformers reveal that the amine lone pair is the HOMO, an out-of-plane π orbital is the LUMO, and the interesting in-plane π orbital is the SLUMO. There is a very large coefficient at the central carbon atom of the SLUMO and at the nitrogen lone pair, with these two orbitals having the correct symmetry for bonding. Pictures of these orbitals are presented in the Supporting Information.

When starting from the ketenimine side **1**, during the second part of the activation barrier, from the inflection point in Figure 2, the ketenimine must undergo partial planarization of the C=C=N−H moiety, as has already been pointed out by Birney.[5a] The TS **2** is not actually planar: the imine N−H bond is somewhat out of plane (*IE* 26° (−154°); *IZ* 32°), reflecting the orientation in the ketenimine **3**. Starting from the side of the ketene **3**, the initially planar N−H bond will be twisted out of plane in the TS **2**. However, the fact that the barriers from the rotational TSs (*sE-A180*) to the 1,3-migration TS **2** are virtually identical for ketenes and ketenimines (Figure 1) indicates that the planarization of the ketenimine is not energetically costly.

The orbital interactions described above typify a pseudopericyclic reaction.[5a,7] In the analogous α-oxoketene-α-oxoketene interconversion (eq 2), no twisting or planarization of an N−H bond is required, but the first part of the activation barrier, the rotation of the migrating amino group into the correct orientation, is still required. One may say that the fact that an *intermediate* **7** is formed in the NMe_2 migration is the consequence of the 1,3-migration barrier lying below the rotational barrier of the dimethylamino group.

Conclusion

The rotation of the migrating amino group into the proper orientation for the 1,3-shift is an important prerequisite for the reaction and constitutes the first part of the activation barrier. If the barrier for the 1,3-shift drops below this rotational barrier, there will necessarily be an intermediate in the migration. This explains the existence of the zwitterionic four-membered ring intermediate **7** in the 1,3-migration of the dimethylamino group in α-oxoketenes **6** (eq 3). The rotational transition

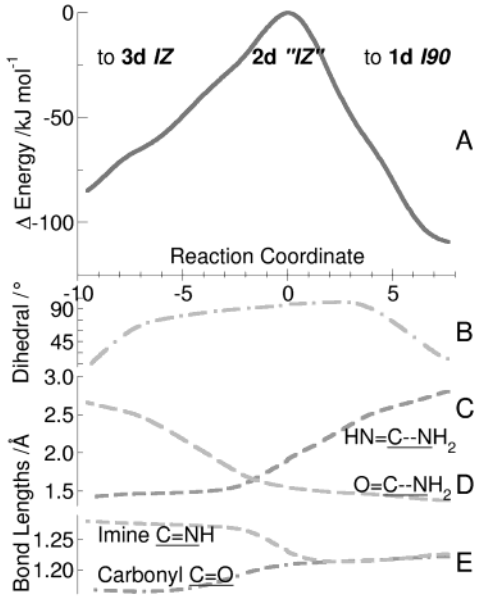

FIGURE 2. NH_2 *IZ* 1,3-migration (between **1d** *I90* and **3d** *IZ*) transition-state intrinsic reaction (IRC) path following calculation. Step size in this calculation was 0.05 units. (A) The energy axis represents the change in energy from the 1,3-migration transition state in kJ mol^{-1}, the values being the B3LYP/6-31G* total energies, with no corrections for enthalpy, etc. applied. (B) The dihedral angle between an NH bond in the migrating NH_2 group and the plane of the molecule (the ground-state angle is ∼30°). (C, D) The distances between the migrating amino group and the imine and carbonyl carbons. (E) The lengths of the imine and carbonyl bonds. All graphs share the reaction coordinate axis, which represents movement along the path of the transition vector. The positive direction is where the largest component of the phase is positive. This vector is calculated in mass-weighted internal coordinates, making the axis units $amu^{1/2}$ Bohr (∼2.16×10^{-24} $kg^{1/2}$ m). Similar graphs for the other three migrations are included in the Supporting Information.

states (*sE-A180* in Figure 1) can be regarded as a pre-transition state for the 1,3-migration lying close to the VRI points (at −6 and +4, Figure 2). At this point there is a strong bonding interaction between the amine lone pair (the HOMO) and a vacant in-plane cumulene π orbital (the SLUMO). This gives rise to the new N−C bond formed in the TS for the 1,3-migration. For the hindered rotation of the amino group (rotation B, Scheme 2), the barrier decreases with increased polarization of the conjugated system (**6a** *sE:* 39; **1d** *sE-kI90:* 49; and **11** *sE:* 54 kJ mol^{-1}). A decrease is also observed for this barrier when going from the *sZ* to the sE conformers (for NH_2 in oxoketenimine **1d** 55 versus 49; for acrylamide **11** 67 versus 54, and for $N(CH_3)_2$ in **1e** 60 versus 44 kJ mol^{-1}). This story is repeated for the amidine cases if we only compare the A180 structures (in the *IE-A0* structures a favorable hydrogen bond causes an increased barrier).

The presence of VRI points either side of the transition state has an intriguing and significant corollary. Increasing the energy barrier for the two underlying transition states and/or reducing the energy of the primary transition state might convert the transition state into an intermediate, as for **7** in the 1,3 migration of NMe_2 in α-oxo-ketene **6b** (eq 3). This gives us a possible route for examining a range of transition state-like structures in the laboratory.

A heterocumulene moiety has a slightly higher effect on the *E*/*Z* rotational barrier (rotation A, Scheme 2) (increase by 4−8 kJ mol^{-1}) than a C=C double bond. This is most pronounced here for the amidine cases, e.g., for imidoylketene **3d** *IZ* 24 versus 17 kJ mol^{-1} for acrylamidine **13** *IZ*. There is a similar difference between the calculated values for the amide rotation in ketene **6a** (26 kJ mol^{-1})[6] and oxoketenimine **1d** *sZ* (24 kJ mol^{-1}) compared to acrylamide **11** *sZ* (20 kJ mol^{-1}). This would suggest that the effect is dependent on the polarization of the relevant double bond (ketene > ketenimine > C=C double bond).

The *E*/*Z* interconversion of the amidine imine group in amidino-ketenes **3** (rotation C, Scheme 2) appears to be independent of the conjugated system. The ketenimine inversion barrier is consistent with results for linear ketenimines[17] where electron-withdrawing groups on carbon reduce the barrier. The inversion barriers for the NH function in ketenimines (35−42 kJ mol^{-1}) are, like the amide/amidine group rotation A, chemically unimportant compared with the 1,3-migration. On the other hand, a complete understanding of the *E*/*Z* interconversion process of the imine NH function in amidines was not achieved. The barriers calculated for an inversion process are similar to those calculated for a rotation process, with the inversion calculated as a second-order saddle point. In contrast, all imines for which this process has been studied appear to prefer the inversion process. This makes amidines an attractive subject for further calculation and experimental study.

Theoretical Calculations

Standard DFT molecular orbital calculations[24] were carried out with the GAUSSIAN 98[25] system of programs. All geometry optimizations have been performed with the standard polarized split-valence 6-31G* basis set[24] at the B3LYP level.[26] Wave function stability and harmonic vibrations (shown as wavenumbers scaled by 0.9613[27]) have been calculated at this level in order to characterize the stationary points as minima or saddle points and to evaluate zero-point vibrational energies (ZPVEs). Improved relative energies have been obtained using the expanded basis set 6-311+G(3df,2p) and the B3LYP method on the previously optimized 6-31G* geometries, the aggregate method being B3LYP/6-311+G(3df,2p)//B3LYP/6-31G*. The enthalpy (ΔH) for the processes was calculated using energy values from the higher level and an unscaled correction from the vibration calculation at the lower level. The entropy (ΔS) was taken directly from the harmonic

(24) Hehre, W. J.; Radom, L.; v R Schleyer, P.; Pople, J. A. *Ab initio molecular orbital theory*; Wiley-Interscience: New York, 1986.
(25) Frisch, M. J.; Trucks, G. W.; Schlegel, H. B.; Scuseria, G. E.; Robb, M. A.; Cheeseman, J. R.; Zakrzewski, V. G.; Montgomery, J. A., Jr.; Stratmann, R. E.; Burant, J. C.; Dapprich, S.; Millam, J. M.; Daniels, A. D.; Kudin, K. N.; Strain, M. C.; Farkas, O.; Tomasi, J.; Barone, V.; Cossi, M.; Cammi, R.; Mennucci, B.; Pomelli, C.; Adamo, C.; Clifford, S.; Ochterski, J.; Petersson, G. A.; Ayala, P. Y.; Cui, Q.; Morokuma, K.; Malick, D. K.; Rabuck, A. D.; Raghavachari, K.; Foresman, J. B.; Cioslowski, J.; Ortiz, J. V.; Stefanov, B. B.; Liu, G.; Liashenko, A.; Piskorz, P.; Komaromi, I.; Gomperts, R.; Martin, R. L.; Fox, D. J.; Keith, T.; Al-Laham, M. A.; Peng, C. Y.; Nanayakkara, A.; Gonzalez, C.; Challacombe, M.; Gill, P. M. W.; Johnson, B.; Chen, W.; Wong, M. W.; Andres, J. L.; Gonzalez, C.; Head-Gordon, M.; Replogle, E. S.; Pople, J. A. *Gaussian 98*, Revision A.6; Gaussian, Inc.: Pittsburgh, PA, 1998.
(26) Becke, A. D. *J. Chem. Phys.* **1993**, *98*, 5648−5652. Lee, C.; Yang, W.; Parr, R. G. *Phys. Rev. Sect. B* **1988**, *37*, 785−789.
(27) Wong, M. W. *Chem. Phys. Lett.* **1996**, *256*, 391−399.

vibration calculation at the lower level. The free energy (ΔG) was then calculated from these two values. The temperature used in the harmonic vibration calculation and hence the thermochemistry was 298.15 K. The thermochemistry presented here includes an (unscaled) correction for ZPVE. A scaling factor of 0.9804 has been recommended for ZPVE/thermal energy calculated using the B3LYP/6-31G* method,[27] but was not applied here, as the difference in ZPVE (ΔZPVE) between two compounds or conformers was expected to be small (<10 kJ mol^{-1}). The corresponding correction for scaling the ZPVE/thermal energy was then estimated at less than ~0.2 kJ mol^{-1}, a value significantly less than the presumed accuracy of the method. The ΔZPVEs have been included in some of the tables in the Supporting Information, so that the interested reader may gain an indication of the error that this lack of scaling may have contributed. The chosen method can be presumed to have an accuracy between B3LYP/6-311+G(2d,p)//B3LYP/6-31G* and B3LYP/6-311+G(3df,2df,2p)//B3LYP/6-31G*. A comparison[28] of these two methods with the experimental data from the GAUSSIAN G2 molecule set had, respectively, mean absolute deviations (standard deviations) of less than 13(12.5) and less than 11(11) kJ mol^{-1}. While the chosen method's overall mean absolute deviation (or accuracy) for predicting energy is estimated at <13 kJ mol^{-1}, the error for closely related compounds would be expected to be smaller. A comparison of the migratory aptitudes of groups in α-oxoketenes **10** calculated using the ab initio G2(MP2, SVP) method[9] with those derived from the DFT method[6] indicated that the latter method overestimates the 1,3-migration barrier for amino groups by only ~3−4 kJ mol^{-1} (Table 1).

Acknowledgment. This work was supported by the Australian Research Council.

Supporting Information Available: A table of the calculated characteristic infrared frequencies for the cumulene, carbonyl, and imine groups; summary figure for the calculated hindered amine rotations; images of the calculated HOMO, LUMO, and SLUMO for **1d** *sE-A180-I90*; companion figures to Figure 2, representing the migration transition state intrinsic reaction (IRC) path following calculation results for the other three cases; summary information for each calculation performed, including Hartree−Fock energy, optimized geometry, calculated harmonic frequencies and imaginary frequencies for transition states. This material is available free of charge via the Internet at http://pubs.acs.org.

JO035419X

(28) Foresman, J. B.; Frisch, Æ. *Exploring Chemistry with Electronic Structure Methods*, 2nd ed.; Gaussian Inc: Pittsburgh, 1995.